

This is an Open Access document downloaded from ORCA, Cardiff University's institutional repository: <https://orca.cardiff.ac.uk/id/eprint/146066/>

This is the author's version of a work that was submitted to / accepted for publication.

Citation for final published version:

Evans, H. P. and Snidle, R. W. 2021. Duncan Dowson: Pioneer of elastohydrodynamic lubrication of gears. Proceedings of the Institution of Mechanical Engineers, Part J: Journal of Engineering Tribology 235 (12), pp. 2592-2603. 10.1177/135065012111053084

Publishers page: <http://dx.doi.org/10.1177/135065012111053084>

Please note:

Changes made as a result of publishing processes such as copy-editing, formatting and page numbers may not be reflected in this version. For the definitive version of this publication, please refer to the published source. You are advised to consult the publisher's version if you wish to cite this paper.

This version is being made available in accordance with publisher policies. See <http://orca.cf.ac.uk/policies.html> for usage policies. Copyright and moral rights for publications made available in ORCA are retained by the copyright holders.



## Duncan Dowson: Pioneer of EHL of gears

H P Evans and R W Snidle

School of Engineering, Cardiff University, Cardiff, UK

### Abstract

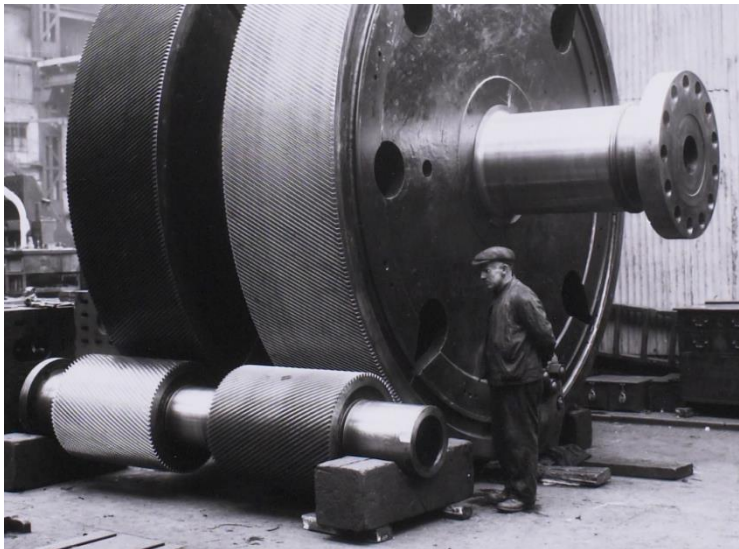
The paper briefly reviews Duncan Dowson's ground-breaking contribution to the theory of elastohydrodynamic lubrication (EHL) in relation to the understanding of lubrication of gear tooth contacts. His early work with Higginson on numerical modelling of EHL finally explained how gears can operate successfully, and avoid wear, due to the generation of a stiff, protective oil film. The resulting minimum film thickness equation stands as a reliable reference formula for calculations in gear design standards. The paper includes examples of how EHL theory has been developed by the present authors and their co-workers, and applied to aid the design of engineering components such as worm gears, thrust rims and profile-modified helical gears. Also included is its extension to include the important effects of surface roughness at the asperity level (micro-EHL) and its relevance to the current, troublesome problem of micropitting.

### Notation

$a$	Hertzian contact semi-dimension for a line contact
$E_1, E_2$	Young's moduli of the two contacting surfaces
$E'$	reduced elastic modulus; $\frac{2}{E'} = \frac{1 - \nu_1^2}{E_1} + \frac{1 - \nu_2^2}{E_2}$
$h$	film thickness
$h_0, h_{\min}$	central and minimum film thickness
$p$	pressure
$p_{\max}$	maximum pressure
$R$	effective radius of curvature at the contact
$U$	entraining (rolling) velocity
$w'$	load per unit width of a line contact
$x, y$	coordinates in the tangent plane of the contact
$\alpha$	pressure coefficient of viscosity
$\eta$	dynamic viscosity
$\eta_0$	dynamic viscosity at zero pressure
$\nu_1, \nu_2$	Poisson's ratios of the two contacting surfaces

## 1. Introduction

Gears have been used for centuries in machines such as windmills, clocks, etc. and are widely applied today in all kinds of vehicles and power transmission systems. They have survived and will be used well into the present century because of their advantage (over alternative methods of transmitting shaft power) of very high efficiency, typically over 90 percent. Gears are not only mechanically efficient, but they have proven over many years to be surprisingly durable in many demanding applications such as the speed-reducing gearboxes in large warships and liners. For example, when the famous Blue Riband liner *RMS Queen Mary* was taken out of service for re-fit, the main propulsion gears (Figure 1) were inspected, and it was found that “...after eleven years’ operation no wear could be detected on the gear teeth.” [1].



National Archives of Scotland

**Fig. 1** Main reduction gears from RMS Queen Mary (one of four sets)

The absence of wear was attributed to the presence of a protective lubricant film, but up to that point there had been little progress in obtaining a theoretical explanation of effective hydrodynamic film generation based on the conventional lubrication theory of Reynolds. An early treatment of this kind was attempted by Martin [2] who believed that “The absence of wear [observed in high speed reduction gearing of the time] must be attributed to the presence of an oil film...”. He assumed that the lubricant was isoviscous and the surfaces remained rigid. On this basis Martin derived the following expression (equation 1) for the minimum film thickness

$$h_0 = \frac{4.90\eta UR}{w'} \quad (1)$$

and the maximum pressure (equation 2) was given by

$$p_{\max} = 2.15\eta UR^{\frac{1}{2}} h_0^{-\frac{3}{2}} \quad (2)$$

The following operating conditions are representative of modern gearing practice and these will be used to compare the predictions of different film thickness formulas as they are encountered in this article.

$$\begin{aligned} \eta &= 0.08 \text{ Pas} \\ U &= 5 \text{ m/s;} \\ w' &= 2 \times 10^6 \text{ N/m;} \\ R &= 25 \text{ mm.} \end{aligned}$$

Assuming these values the film thickness predicted by Martin's formula is  $2.45 \times 10^{-8}$  m (i.e.  $0.0245 \mu\text{m}$ ) and the maximum pressure is 35.5 GPa. Both values require comment. In practice even the best quality gear teeth (in aerospace practice, for example) rarely have surfaces finished to a roughness standard better than  $0.4 \mu\text{m}$  RMS, and such surfaces will have asperities with peak/valley dimensions of, typically,  $4 \mu\text{m}$ . Under these conditions it would seem impossible to provide an effective hydrodynamic film capable of separating real engineering surfaces. Furthermore, the theoretical maximum pressure of 35.5 GPa is far higher than the hardness of even the strongest heat-treated steels used in gears and roller bearings. In retrospect it is clear that the major shortcomings of Martin's analysis were his neglect of load-spreading due to elastic deformation, and the dramatic (approximately exponential) increase in viscosity of oil at high pressure, i.e. the Barus relationship (equation 3).

$$\eta = \eta_0 \exp(\alpha p) \quad (3)$$

A major advance in formulating a theory which combined the two effects was published by Grubin [3] following earlier work by Ertel in what might be described as a lubricated Hertzian contact. A parallel film in the Hertzian contact zone is assumed and the corresponding Hertzian shape of the surfaces in the "gap" in the region outside the contact. By carrying out an integration of the Reynolds equation in the gap or "inlet" region under

entrainment conditions for a range of loads, the following formula (equation 4) for the film thickness in the assumed parallel gap was obtained.

$$\frac{h_0}{R} = 1.95(\eta_0 U \alpha)^{0.727} R^{-0.636} (E' / w')^{0.091} \quad (4)$$

Substitution of the operating conditions used earlier, together with typical elastic constants for steel ( $E_1 = E_2 = 200$  GPa and  $\nu_1 = \nu_2 = 0.3$ ), and  $\alpha = 2 \times 10^{-8}$  m<sup>2</sup>/N gives a film thickness  $h_0 = 1.90 \times 10^{-6}$  m (1.90  $\mu$ m) and a maximum Hertzian pressure of 1.68 GPa.

Given the assumptions made it is clear that Grubin/Ertel formula is meant to apply to what may be described as “heavily-loaded” conditions in which the elastic deformation is large compared to the film thickness, and it did not anticipate the “pressure spike” at the exit from the contact which appeared in subsequent detailed computer models.

In 1959 two young lecturers of mechanical engineering at Leeds University, Duncan Dowson and Gordon Higginson, published their breakthrough paper on a full numerical treatment of the “elastohydrodynamic lubrication” problem [4]\*.

The pair soon realised that a straightforward iteration along the lines of: assume film  $\rightarrow$  calculate pressure from the Reynolds equation  $\rightarrow$  calculate elastic deformation  $\rightarrow$  adjust film shape  $\rightarrow$  recalculate pressure, etc. was unstable. Their key to overcoming this problem was the introduction of an approach in which a film shape was obtained corresponding to an assumed pressure rather than the other way around. This “inverse” treatment of the Reynolds equation (which involves the solution of a cubic equation in the case of a line contact) led to a stable iterative process. The then head of department at Leeds described this as “relaxation proper”, but the young lecturers preferred to call it “relaxation improper” [5]. Their results were obtained on a relatively coarse finite-difference grid (using desk calculators!) and although an exit constriction was evident in the solutions shown, the conditions did not give rise to the “spike” as predicted earlier by Petrusevich [6]. .

Later solutions [7] obtained over a wider range of operating conditions with the aid of a digital computer showed the spike, which significantly exceeded the corresponding Hertzian pressure maximum under high speed conditions. The spike was eventually confirmed experimentally in a brilliant paper by Hamilton and Moore [8]

---

\* Some fascinating historical details of Dowson and Higginson’s early efforts in the pre-computer period of numerical EHL, including an encounter with Petrusevich, are given in a paper presented by them at a Cardiff symposium 45 years later [5]]

Based on their early results Dowson and Higginson [9] gave a formula for the *minimum* film thickness (which occurs at the exit constriction) as follows (equation 5).

$$h_{\min} = 1.6 \frac{\alpha^{0.6} (\eta U)^{0.7} (E')^{0.03} R^{0.43}}{(w')^{0.13}} \quad (5)$$

The close similarity to Grubin's formula may be noted. Substitution of the operating conditions stated earlier gives a *minimum* film thickness of 1.4  $\mu\text{m}$ . The minimum film thickness in Dowson and Higginson's solutions was typically about 75% of that in the parallel section of the film, so the agreement with Grubin's prediction (which relates to the parallel section) is good, and this underlines the essential validity, for engineering calculations, of Grubin's model of the heavily-loaded EHL contact and the assumptions on which it is based. In 1966 Dowson and Higginson published their well-known book on elastohydrodynamic lubrication [10] which included an updated minimum film thickness formula including its application to an example of spur gear contact conditions. Subsequently Dowson and Toyoda [11] provided a separate formula for the *central* film thickness for line contacts. By the mid 1960s the essential features of EHL were well understood and a workable film thickness formula had been largely validated as a result of the experimental work of Dyson, Naylor, and Wilson [12]. Dowson and Higginson's work triggered a massive academic interest in EHL leading to refinements including thermal, non-Newtonian, point contact and traction studies. The isothermal film thickness formula remains, however, as an accepted equation of engineering science, and provides a reliable reference value for calculations in industry, particularly in relation to the roughness of gear teeth in design standards.

Researchers at Cardiff were one of the many groups influenced and encouraged by the publications of Duncan Dowson on EHL. Their work has included basic contributions to point contact theory and experimentation, and has developed into a strong specialisation in gear lubrication and durability. The following sections describe some examples of how we have applied EHL analysis to solve some practical gear lubrication problems.

## 2. Examples of the application of EHL analysis to gear lubrication problems

### 2.1 What EHL theory means to gearing and traction drive applications.

EHL theoretical advances stemming from Dowson and Higginson's work have provided design tools for gear and traction drive applications that give a rigorous basis for estimates of elastohydrodynamic film thicknesses in those devices. The formula does not give the whole story, however, because of a number of complicating factors in these applications.

(i) Lubricant properties. These are summed up in the EHL formulae as the ambient pressure absolute viscosity,  $\eta$ , and the pressure-viscosity coefficient,  $\alpha$ . In a general application neither of these are known as functions of temperature. For any commercial lubricant the kinematic viscosity is specified at temperatures of 40°C and 100°C and the density may be specified at 15°C. Use of the ASTM method [13] gives a means to determine the kinematic viscosity at different temperatures and the thermal expansivity can be used to obtain the required absolute viscosity.

The pressure viscosity coefficient is a different matter with no general measured values being available for commercial products although there are values given for some Mobil products [14], and there are correlations with kinematic viscosity such as Wu et al, [15].

(ii) To specify the lubricant properties for steady state conditions some knowledge of the contacting component temperatures is required. This is because the EHL lubricant film is generated in the inlet to the contact, in the close vicinity of the Hertzian contact area boundary. The surface temperatures of the contacting bodies in this inlet zone determine the inlet temperature as was established experimentally by Crook [16] which means that neither the sump temperature or the lubricant supply temperature to the contact give the appropriate viscosity value required for EHL calculations, although they are often thought to do so. The variation in  $\eta$  and  $\alpha$  for a commercial lubricant determined using references [13] and [15] are shown in Figure 2 and indicate the sensitivity of the parameters to temperature.

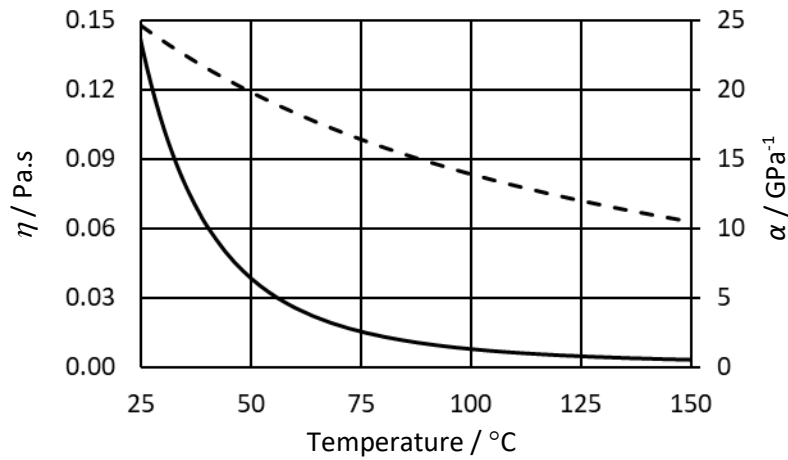


**Fig. 2** Variation of viscosity (solid) and pressure viscosity coefficient (broken) determined from lubricant datasheet.

(iii) Thermal effects. For contacts operating in pure rolling conditions where the contacting surfaces move relative to the contact point with equal or near equal velocities there are no significant sliding effects. This is the case in rolling element bearings, for example, but is hardly ever the case in gear and traction drive applications. When sliding is significant the EHL problem becomes a thermal problem and the dissipation of energy within the shearing lubricant film and the transport of heat within the film and to the contacting bodies takes the problem beyond the realm of the Dowson and Higginson formula. For EHL contacts subject to significant sliding designers may need to estimate the power loss in the contact. This introduces the additional complication of the appropriate rheology to adopt in modelling the heat dissipation, with numerous models having been proposed, each of which introduces further property parameters that control the shear stress/ shear strain rate behaviour of the lubricant.

## 2.2 Worm gears

Worm gears (Figure 3) provide a simple and cost-effective solution where high reduction ratios are required in relatively slow speed drives.

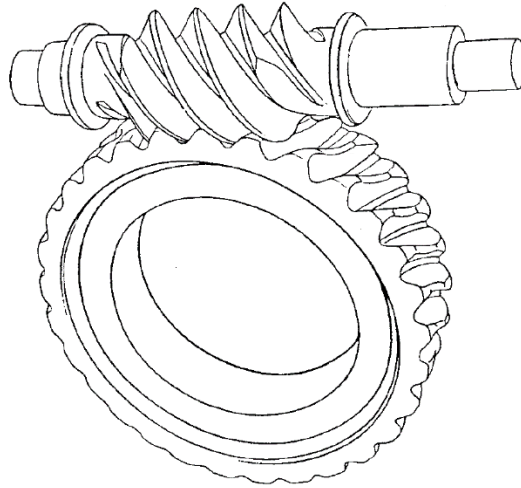


**Fig. 3** A pair of worm gears

The main disadvantages of worm gears are lubrication and wear problems due to the high degree of sliding at the tooth contacts. In order to avoid scuffing the worm and wheel components are made from materials of dissimilar metallurgy, usually steel for the worm and phosphor bronze for the wheel. The use of a relatively soft material for one of the components limits the allowable contact stress and hence load capacity and corresponding power to weight ratio of the drive. The high sliding leads to poor efficiency of typically 70-80 percent, which may be compared to that of conventional spur and helical gears of 95 percent or better. Worm gears take different forms. The most common type is the “ZI” specification in which the worm is an involute helicoid and the wheel is generated using a hob which is nominally of the same shape as the worm. If the hob and worm are of exactly the same shape then the contact action is conjugate, and contact occurs along a line. However, this prevents effective lubrication as entrainment is directed along the line of contact and the required “inlet wedge” is absent. In order to overcome this problem the hob is, in practice, chosen to be oversize, which, under load, produces a roughly elliptical contact with oil entrainment nominally in the direction of the major axis of the contact. Even with this refinement, however, the hydrodynamic film-forming conditions are relatively poor because of the unavoidable high slide/roll ratio. The starting point for an EHL analysis of worm contacts is the generation of the non-conjugate shape of the wheel surface. A digital technique for this purpose was described by Hu [17] a gear expert at Newcastle University.

The geometry data provided in this way was first smoothed by fitting high-order polynomials (up to order ten) to the numerically-provided data to give a continuous mathematical equation for the shape of the surfaces. An example is shown in Figure 4 which is a projection into the plane perpendicular to the worm axis containing the wheel axis. This approach avoided what amounted to “roughness” in the raw numerical data due to precision issues at the level of the film thicknesses expected.

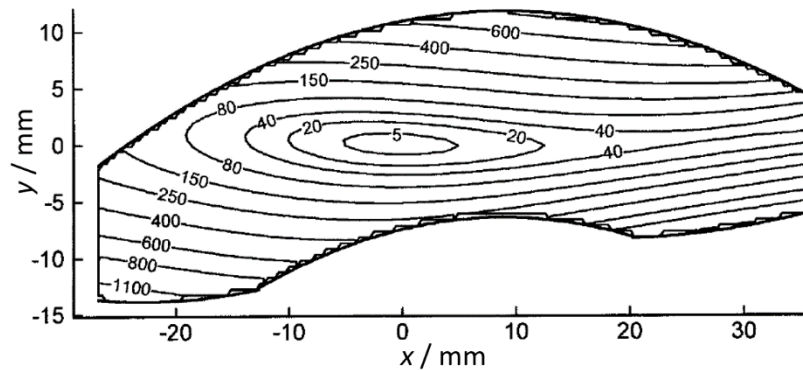


**Fig. 4** Contours of gap between worm and wheel teeth ( $\mu\text{m}$ ) when the point contact is at coordinate position (0,0).

Full EHL analyses of film generation in a wide range of sizes of practical gear pairs (a total of eight different designs) was carried out. An essential feature of the analyses for worms was the detailed treatment of the kinematics of lubricant entrainment to take account of the fact that the tangential velocities of the two surfaces varied continuously from point to point over the whole area of film generation. This behaviour is illustrated in Figure 5 which compares the entrainment vectors for two different designs at the two extremes of scale, and worm tooth numbers (threads) of the designs considered.

In the upper part of the figure, which corresponds to a relatively small gear pair ((a) single thread 17 mm diameter worm) the dry contact area is close to elliptical in shape, but in the lower part a much larger pair with multiple threads ((b) four thread 130 mm diameter worm) shows a markedly distorted, banana-shaped dry contact, and in this case the entrainment vectors vary considerably in direction relative to the contact, being almost in line with the elongated contact at the inlet region, but veering to being almost transverse to the contact towards the exit. This leads to unusual patterns of film generation as will be seen. In view of the high sliding present in worm contacts a full thermal treatment was included together with non-Newtonian behaviour of the lubricant. The detailed formulation of the EHL solver has been described in detail in previous articles [18,19].

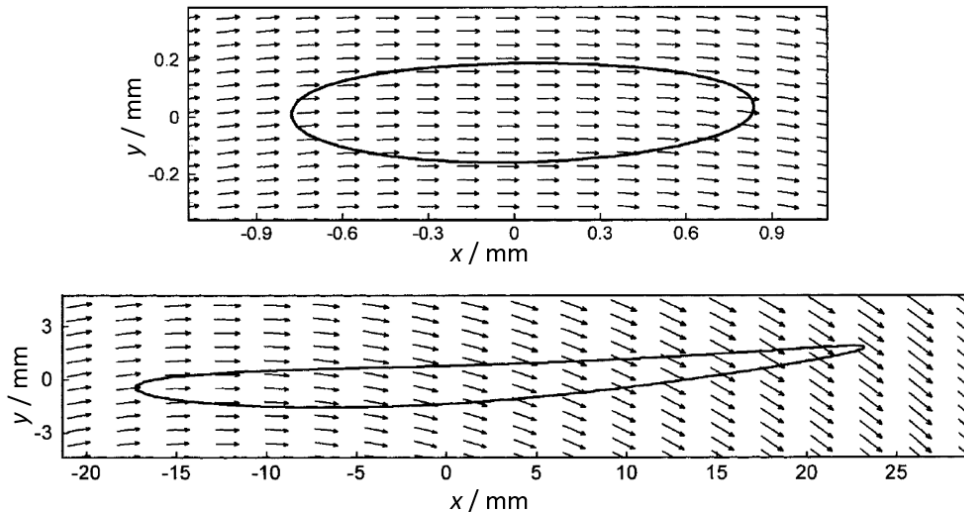


**Fig. 5** Dry contact area and entrainment velocity vectors when the point contact is at coordinate position (0,0) for designs (a) and (b).

Figure 6 shows typical results obtained from the thermal EHL analysis of the pair shown in the lower section of Figure 5. The condition considered corresponds to Figure 5b where contact occurs roughly half way up the wheel tooth. The figure shows contours of film thickness together with the mid-film lubricant temperature for an assumed inlet temperature of 60 °C. These typical results confirmed that EHL films, of the order of about 1  $\mu\text{m}$  can be formed in worm gear contacts, but that sliding leads to the generation of significant thermal effects with the mid film oil temperature rising to a maximum of 130 °C in this example with the maximum tooth surface temperature reaching 120 °C.

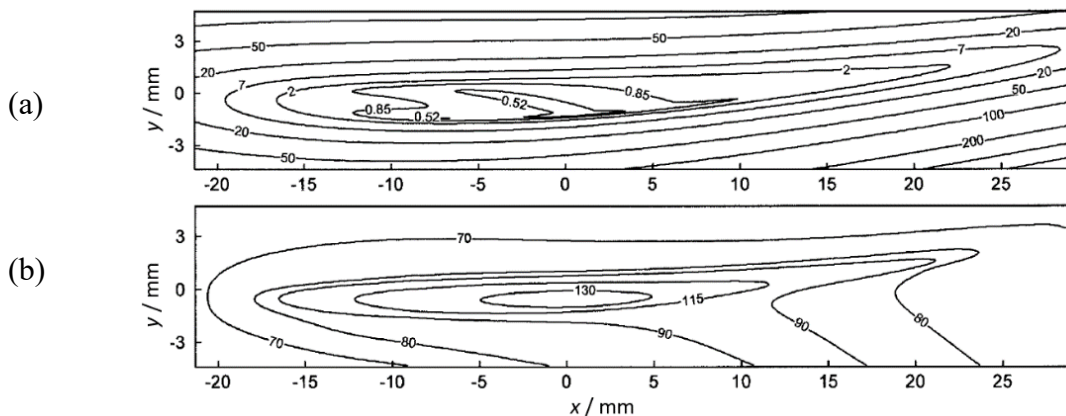


**Fig. 6** Contours of (a) EHL film thickness /  $\mu\text{m}$  and (b) mid lubricant plane temperature / °C obtained from a thermal EHL analysis for design (b) with contact at position shown in Figure 5b.

## 2.3 Thrust cones

Thrust cones (or thrust rims) are used to react the axial force produced in a pair of *single* helical gears. They take the form of overlapping conical rims placed on the edges of the gears as shown schematically in Figure 7.

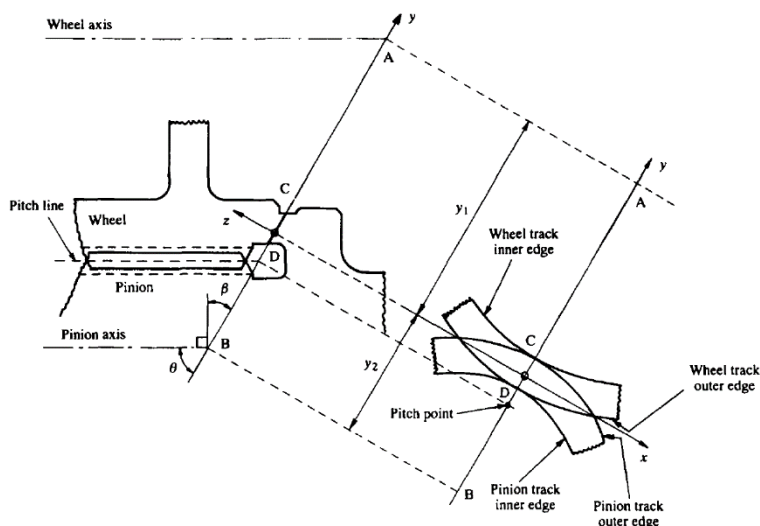


**Fig. 7** Basic thrust cones geometry showing the overlap area. The left hand diagram shows the transverse section of the wheel and pinion with contact between the thrust cones along the line CD. On the right is a projection of the thrust cone edges into the common tangent plane at the line of contact.

Lubrication of the line contact between the cones takes place in the area of overlap between the rims. Thrust cones have particular advantages in large, high-power reduction units such as those in naval applications where weight is an important factor. By reacting the axial thrust force more or less in line with the contacting teeth (i.e. close to the pitch line of the gears) the load path via the flange of the larger gear is avoided, leading to low distortion and good alignment of the mesh. It should be noted that although double-helical (“herringbone”) gears (Figure 1) also deal with the thrust problem, and are the traditional solution for large reduction units, it turns out that single helical gears with thrust cones provide a far simpler solution, leading to a lighter gearbox, and, crucially in naval applications, lower noise. Large single helical gears with thrust cones have recently been successfully used in important naval vessels.

By using a low cone angle (typically of the order of 1 degree) the geometrical conformity in the entraining direction can be relatively large (of the order of metres in large units) and the potential exists for the generation of an effective lubricant film. In early designs purely

conical rims (resulting in a line contact) were used, but this arrangement relied on precise matching of the two cones in order to avoid edge contacts. In practice perfect alignment was not possible, and EHL analysis of purely conical rims [20] showed that although healthy films of the order of 10  $\mu\text{m}$  could be theoretically generated over most of the overlap area between the cones, the film at the edges of the un-relieved line contact effectively collapsed, leaving the possibility of scoring damage to the surfaces. Typical results of a full EHL analysis of the finite-length line contact between pure cones showing severe thinning of the film at the edges of the overlap area are shown in Figure 8.

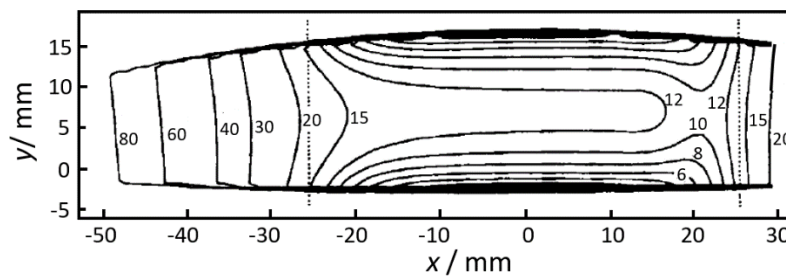


**Fig. 8** Contours of calculated film thickness /  $\mu\text{m}$  for contact between pure thrust cones. Contours for 4, 2 and 1  $\mu\text{m}$  are present in the side lobes where minimum films as low as 0.2  $\mu\text{m}$  occur.

Crowning one of the cones in the radial direction gives a natural self-aligning, nominal point contact which can tolerate the inevitable distortions and manufacturing errors present in practice [21]. Crowned thrust cones have since been applied successfully in important naval main propulsion gearboxes.

As in the case of worm gears the starting point of the full EHL analysis of crowned thrust cones was the definition of the geometry and kinematics in the region of film generation.

Figure 9 shows the unloaded contours of the gap between a pair of crowned cones.

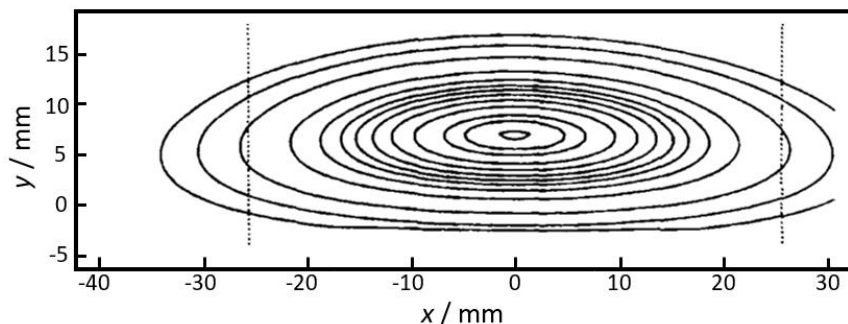


**Fig. 9.** Contours of the gap between a pair of thrust cones with nominal point contact at  $x = 0$ ,  $y = 6.9$  mm. Co-ordinates  $x$  and  $y$  are in the tangential and radial directions, respectively.

Contours shown are for 0.1, 1, 2, 4, 6, 8, 10, 12, 15, 20, 30, 40, 50  $\mu\text{m}$ , and broken lines indicate line contact limits of Figure 8.

In this typical case of a large naval reduction pair the contours indicate that the corresponding contact is of almost elliptical shape with entrainment in a direction roughly along the major axis of the contact. The full EHL analysis of such contacts was similar to that formulated for worms described above. In comparison to worms, however, the degree of sliding is generally much lower, so in initial work we assumed isothermal conditions. Figure 10 shows contours of film thickness at full design load (axial thrust force of 151.8 kN) for a typical large unit.

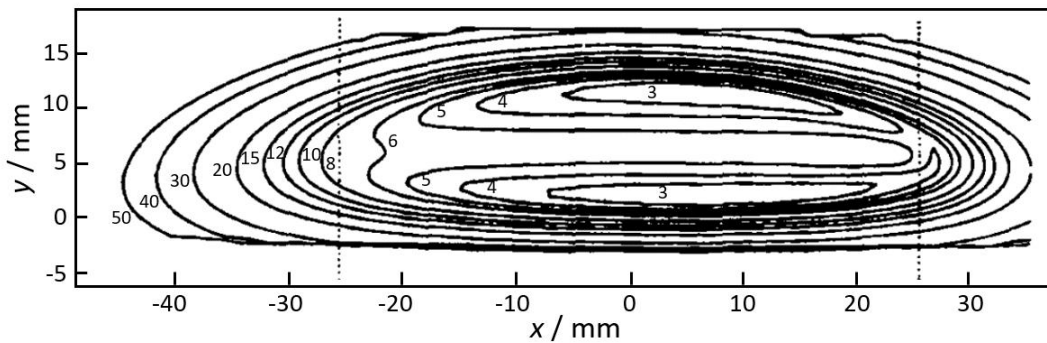


**Fig. 10** Contours of EHL film thickness /  $\mu\text{m}$  for the thrust cones of figure 9. Central film thickness is  $5.7 \mu\text{m}$  on  $y \approx 6.5 \text{ mm}$  for  $x$  between  $\pm 15 \mu\text{m}$ . The minimum film thickness is  $2.17 \mu\text{m}$  and occurs in the side lobes.

The cones rotate about their axes (the gear axes) which are located on line  $x = 0$  and entrainment is in the positive  $x$  direction on  $x = 0$ . In this case a minimum film thickness of  $2.17 \mu\text{m}$  is predicted with a central value of  $5.71 \mu\text{m}$ . Thus although some sacrifice of maximum clearance occurs compared to that predicted for the same conditions using purely conical rims, this is far outweighed by a proper minimum clearance. Given the size of the gears required to transmit the required power over a range of speeds (diameter and face-width of gears, tooth module, materials, etc) the remaining choices for the designer are the thrust cone angle and the radius of the crowning. A low cone angle is chosen to provide good entrainment, and the crowning is optimised to make full use of the width of the overlapping tracks. Clearly the contact area at full load should remain safely within the overlap width under conditions of calculated maximum misalignment otherwise the contact would run over the edges of the tracks, and the benefits of crowning lost. The means of optimising a competitive thrust cones design was provided to the industrial sponsor in the form of a “Thrust cones design aids” (TCDA) package which was initially based on the results of isothermal EHL analyses, but was later updated to include thermal effects arising from sliding within the contact.

## 2.4 Helical gears

Involute helical gears are the most commonly used type for power transmission applications and are adopted for their inherent smoothness in operation in comparison with spur gears. (The simplicity of spur gears is obtained at the cost of transient loading effects as tooth pairs come into and out of contact). For involute teeth the contact is a line contact inclined at the helix angle to the axial direction. For parallel axis helical gears each axial section makes contact at a different point in the meshing process of the involute gear profiles due to the helical action. Under zero load the teeth make contact along a straight line and have the characteristics of a Hertzian line contact. A pair of teeth comes into contact progressively. The contact starts in the root of the pinion (driver) where its limits are determined by the face boundary and the tip of the wheel tooth. The length of the line contact grows subsequently until it occupies the full face width. Full face width contact continues until the contact line first crosses the tip of the pinion tooth. The contact line then progressively reduces in length until the teeth move out of mesh. To minimise impact loading as teeth come into mesh some form of profile modification at the tip of gears is common. The radius at which this tip relief is first applied then determines the start and end of the active profile contact rather than the tips of the gears. To avoid edge effects and the stress concentrations and EHL film thinning that would occur at the face boundary some form of edge relief is customary.

The radius of relative curvature of the contacting surfaces varies along the line of contact according to the distance of the point on the contact line from the line of centres of the gears measured normal to the contacting surfaces. So the line contact has a varying radius of relative curvature in the lubricant entrainment direction ( $R$  in above equations) and also a radius of relative curvature perpendicular to the entrainment direction that becomes significant at the ends of the line contact.

In spite of the unquantified departures of the helical gear contact geometry from the classical EHL line contact of equation (2), it is the primary tool used to estimate film thickness as can be seen from reference to the gear design standards in Europe and the USA. This is because (i) it is the best available straightforward tool and (ii) the EHL process is a very robust (stiff) film forming mechanism. The EHL formula gives a good estimate of the order of film thickness between the contacting gear teeth. It does not identify the level of departure from this value at the ends of the contact line. The edge relief and/or tip relief changes to geometry must be effective at the scale of the EHL film generated. A simple chamfer would be

geometrically far too abrupt, and has no influence on relieving the edge contact, serving only to reduce the effective face width while generating significant edge stress concentrations. Figure 11 illustrates the effects of tip and edge relief on the EHL pressure and film thickness at three different positions, 13%, 52% and 86% of the tooth contact cycle for a pair of involute gears with module 4.5 mm, reference helix angle  $19.6^\circ$ , centres distance 160 mm, and a tip relief of  $70\ \mu\text{m}$  over 2 mm.

For case (a) the contact line covers about half of the face width and is mainly in the dedendum of the pinion, which is the driving gear. Case (b) is in the mid contact position with the contact line covering the full face width of the gear. Case (c) is towards the end of the tooth contact cycle with the contact line in the pinion addendum. Note that the  $x$  and  $y$  axis scales for the film thickness contour plots are in the ratio 40:1 with case (b) having a contact line covering all of the face width. This contact would have a dry contact area about 44 mm long and 0.46 mm wide corresponding to the green/light blue contour boundary. It has the characteristics of an EHL contact with a near constant film thickness of around  $0.27\ \mu\text{m}$  over the area that develops a significant EHL pressure. Lubricant entrainment is in the positive  $x$ -direction and the characteristic exit constriction can be seen as the yellow contour band at the exit to the dry contact zone at around  $x = 0.22\ \text{mm}$ . EHL analysis using equation (2) would be carried out using the radius of relative curvature at the pitch point and would give a good picture of what emerges in this detailed transient analysis [22] with the exception of the ends of the contact line.

The minimum film thickness occurs at the side boundaries where distinct side lobes can be seen with a reduction of up to 40% in the film thickness compared to the central value of  $0.27\ \mu\text{m}$ . The side lobes are similar to, but more severe than, those that occur in a high aspect ratio elliptical EHL contact with entrainment in the minor axis direction. Their inclination to the  $x$  axis is due to the inclination of the contact line to the face boundaries that occurs in helical gears.

For cases (a) and (c) the contact line is reduced in length and constrictions occur centred at  $x = 0, y = 8\text{mm}$  for case (a) and at  $x = 0.15\text{mm}, y = -2\text{mm}$  for case (c). These constrictions are at the ends of the contact line where it passes into the tip relief zones for the wheel in case (a) and the pinion in case (c). The constrictions at the other ends of the contact lines are at the face boundaries and appear to be less aggressive than those of case (b).

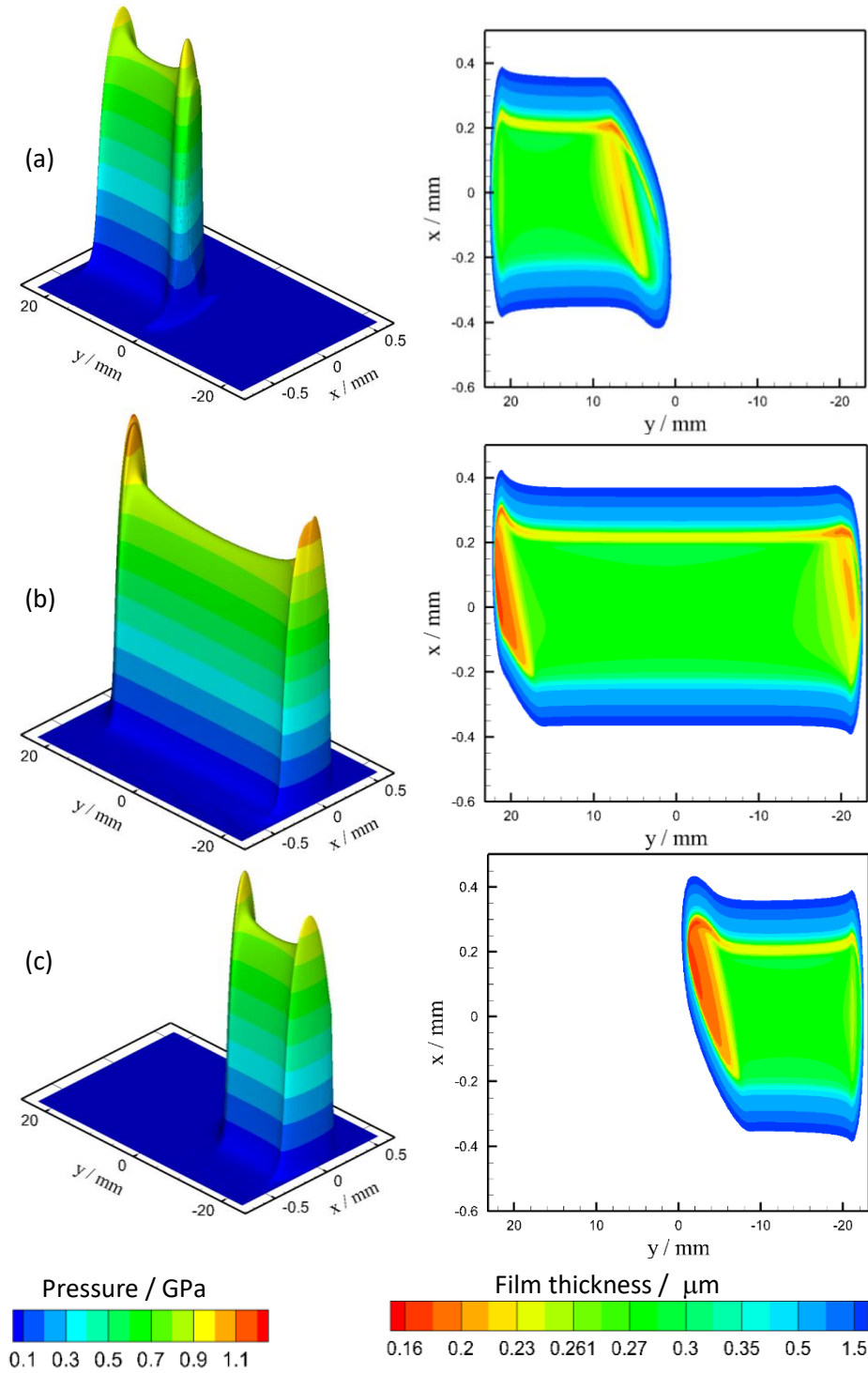


**Fig. 11** Pressure and film thickness contours for a helical gear at three different timesteps in a transient EHL analysis (a) early, (b) mid and (c) late in the tooth meshing cycle, where  $x$  is the entrainment direction and  $y$  is the contact line, Jamali [21].

The considerations above are based on gear tooth geometries that are defined analytically in terms of involute profiles and geometric relief profiles. Power transmission gears are typically made of hardened steel surfaces for resilience and to sustain high contact pressures. This usually involves hardening of the materials, and the final shape of the tooth flanks is achieved by a grinding process. This results in a surface finish that deviates from the analytic form assumed for theoretical analysis. These deviations may be removed by a super-finishing process so that the gear flank reverts to an analytic form with surface roughness  $R_a < 10 \mu\text{m}$ , but are generally accepted as a feature of gear manufacture with the additional process of superfinishing being reserved for special applications that justify its cost. The deviations in form are assessed and controlled using gear profile contact measuring equipment which plots root to tip profiles of deviation from the ideal involute profile. An example of such a profile is given in Figure 12 where the material is below the trace in this view. The gear root is to the left of the figure and the tip to the right. The dashed blue line is a best fit line for the trace between the marker bars which denote the limits of the involute profile. The true involute curve would be parallel to the horizontal grid so that the slope of the fitted line indicates the error between the measured trace and the true involute. The deviations from this line indicate the localised form errors of the manufactured gear.

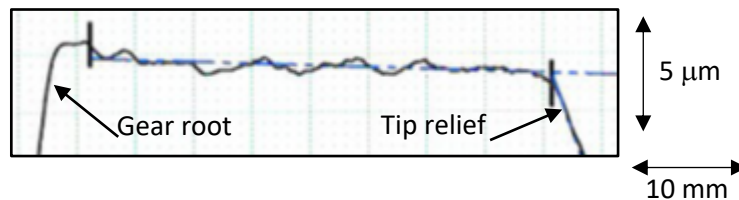


**Fig. 12.** Trace obtained from involute profile testing machine.

The profile deviations measured have features with peak to valley height differences of the order  $1\mu\text{m}$  over a 5 mm trace length and as such are regarded as involute form errors rather than surface roughness features. Using the measured form errors for a pair of meshing gear teeth in an EHL analysis [23] shows their influence on the pressure and film thickness values obtained as illustrated in Figure 13 which has the same 40:1 ratio for the  $x$  and  $y$  coordinate scales as was the case in Figure 10.

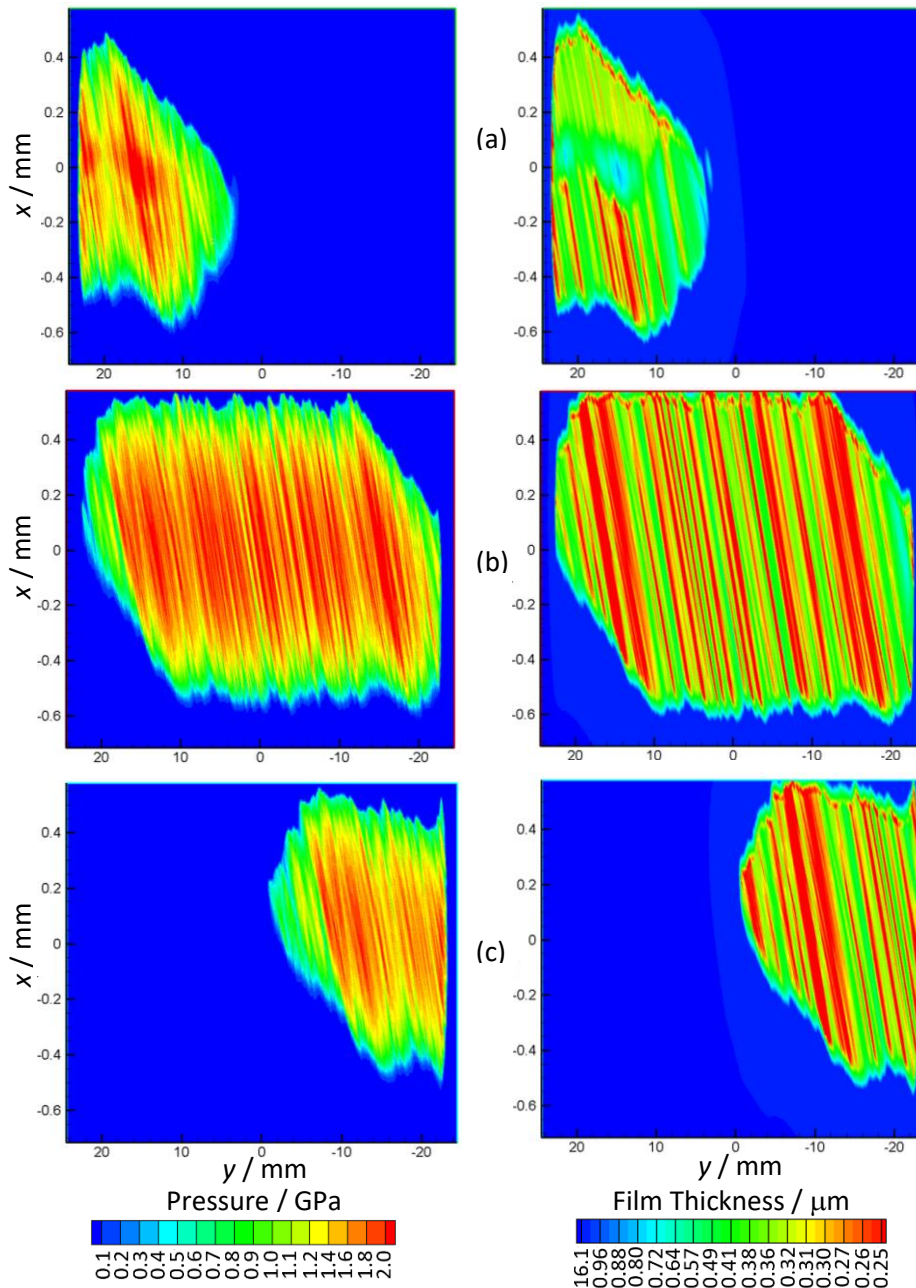


**Fig. 13** Pressure and film thickness contours for a helical gear pair (a) early, (b) midway and (c) late in the tooth meshing cycle. Measured profile errors for the meshing tooth flanks included in the EHL calculation.

The effects of the profile errors on the EHL results are very apparent. The film thickness figures show a series of undulations in the lubricant film. These appear to pass from the inlet to the exit zone at about  $9^\circ$  to the  $x$ -axis, but when the aspect ratio of the  $x$  and  $y$  scales is

considered they are actually orientated at  $9^\circ$  to the  $y$ -axis. Careful inspection of larger scale contour plots show that deviations consist of two families of almost parallel features and these correspond in orientation to the visible grinding marks on the surface.

The variation of contact pressure within the dry contact area is now considerable with values cycling between 1.2 GPa and 2 GPa along the  $y$  axis of each case shown and the classical EHL concept is now swamped by deviations generated by the form errors. It is worth noting that the measured deviations correspond to ISO 1328 Class 5 gears.

### **2.5 Micro-EHL and contact fatigue**

Having considered the effect on the EHL film of form errors on in-tolerance gears it is worth considering the effect of the much smaller departures from smoothness that correspond to surface roughness. The lay of roughness on a helical gear flank depends on the manufacturing process used to finish the hardened gears but it is generally near to the axial direction. A suitable first approximation model to study the effect of roughness is of a line contact whose surface roughness is extruded perpendicular to the entrainment axis. This allows the resolution of surface roughness to be sufficiently fine to capture the first order effects.

The complication in EHL calculations of this model is that the problem becomes intrinsically highly transient as both surfaces are moving relative to the nominal line contact which is the origin of co-ordinates for the Reynolds equation that governs the pressure in the lubricant film. This means that the roughness profiles of each surface are moving relative to the coordinate axes so that the undeformed shape of each surface is time dependent. Surface asperity features on both surfaces process steadily through the Hertzian contact zone and asperity features on the faster moving surface overtake features on the slower moving surface in a systematic way. When this happens within an EHL oil film a micro-EHL oil film is generated that prevents asperities actually colliding with each other, or at least attempts to do so. Whether or not the micro-EHL mechanism succeeds in maintaining separation depends on the shapes of the asperities as well as the other factors influencing EHL film generation. The results of such an analysis is a series of timesteps for which pressure and film thickness distributions are obtained from simultaneous solution of the Reynolds equation and the elastic deflection of the two surfaces. Figure 14 shows the result for one such timestep. This is taken from a transient analysis of the interaction between portions of teeth that engage with each other during the tooth contact cycle. The contact considered is at the onset of single tooth

contact where the sliding speed is high. The figure shows the calculated EHL pressure,  $p$ , and film thickness,  $h$ , distributions together with the two deformed rough surfaces,  $h_1$  and  $h_2$ , in their contacting positions. The rough surfaces are offset by  $10\ \mu\text{m}$  and scaled by a factor of 3 in the figure for clarity.

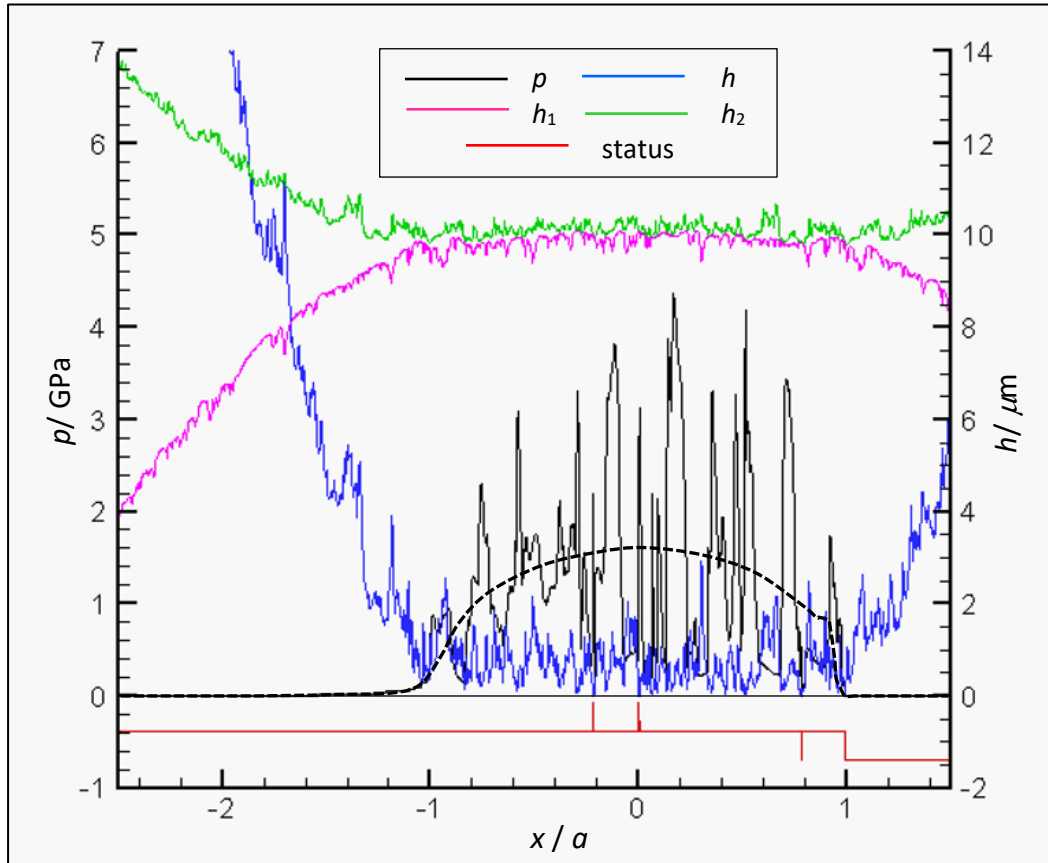


**Fig. 14** Results for a timestep in the transient EHL analysis of two measured roughness profiles that interact during the tooth contact cycle

The red status indicator at the bottom of the figure has three possible levels. The mid level indicates a micro-EHL film separating the surfaces, the lower level indicates any mesh points for which the film is cavitating, and the upper level indicates any points where the micro-EHL film is unable to separate the surfaces during the timestep with direct contact of the surfaces occurring. This timestep is chosen as an example because it has direct contacts at  $x = -0.202a$  and  $x = 0$ , and a localised cavitation event at  $x = 0.79a$ . Here  $a$  is the corresponding line contact Hertzian dimension, and the cavitation occurring in the exit zone where  $x > a$  is a natural feature of all EHL films that cavitate as they pass into the divergent exit zone.

The broken curve shows the corresponding smooth surface pressure distribution with a peak value of 1.6 GPa at  $x = 0$ . Clearly, including the real roughness in the analysis leads to a radically different result than that predicted by the classic EHL theory with peak pressures of up to 4 GPa developing due to micro-EHL at asperity interactions.

Asperity features can be seen to experience intense concentrated high pressure loading and this leads to plastic deformation of the asperities which is the running-in process at work in ground gear contacts when they are first put into service. The profiles used in Figure 14 have gone through the running-in stage and represent the stable surface finish during prolonged running. As such, prominent run-in asperities will experience a number of intense loading-unloading cycles each time that they pass through the EHL contact. This intense cyclic loading can be considered as a potential cause of surface fatigue leading to near-surface micropitting which is a cause of gear flank wear and failure.

Using the critical plane shear strain rate fatigue model proposed by Fatemi and Socie [24] as outlined by Qiao et al. [25] the number of gear rotation cycles to fatigue can be calculated and the results of such an analysis are illustrated in Figure 15

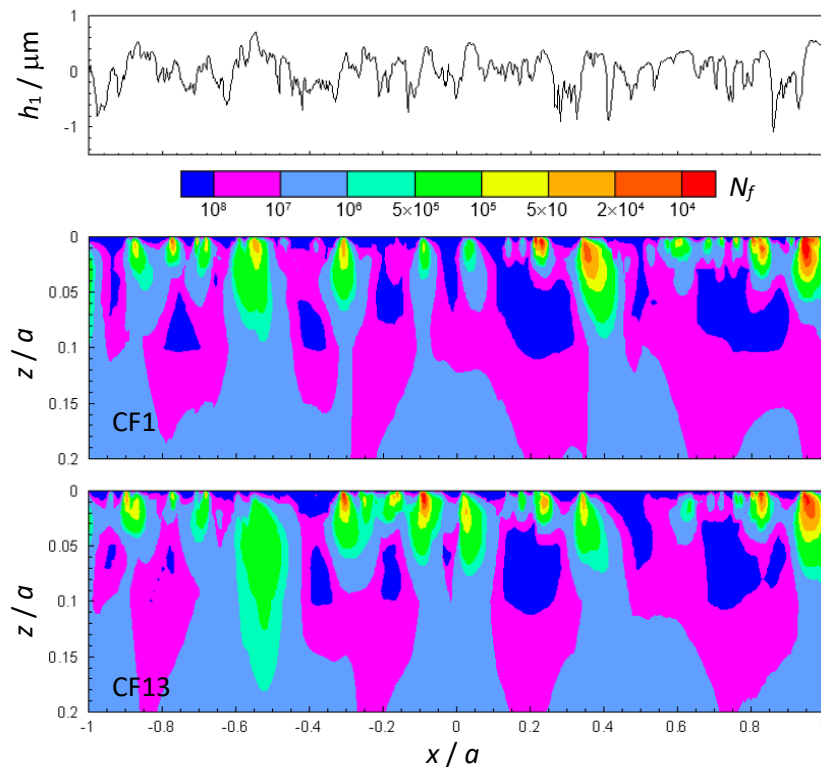


**Fig. 15.** Roughness profile and calculated fatigue lives due to EHL contact with counterface roughness profiles taken from two of its meshing gear teeth.

The upper frame of the figure shows a test roughness profile taken from a gear test for EHL analysis. The gears used in the test had a hunting ratio. Two analyses were carried out using counterface profiles taken from two teeth of the meshing gear, denoted CF1 and CF13 here. In each analysis the kinematic conditions correspond to the actual relative motion and interaction of the profiles as the test gears rotate under load. The surface loading history obtained from the transient micro-EHL analyses was then used to calculate the accumulated fatigue damage for passage of the test profile through the gear contact. The fatigue results are given in the form of contour plots of the calculated number of meshing cycles to fatigue,  $N_f$ , and show how this varies beneath the surface. Coordinate  $z$  is the depth into the material, and the spatial axes are scaled by the nominal Hertzian contact dimension,  $a$ , which is 0.44mm for this example.

The contour plots show how the instances of high calculated damage occur within 15  $\mu\text{m}$  of the surface. The high values generally correspond to prominent asperities on the test profile. In this example the results for interaction with counterface CF1 are quite similar to those for interaction with CF13, but this is not always the case as the peak pressures which drive the fatigue calculation are a product of the interaction of asperities.

### **3. Conclusion**

Duncan Dowson was a great pioneer in the study of lubricated contacts. In his early work with Higginson the importance of EHL in gearing was well appreciated. The fact that the teeth of gears had operated, trouble free, for many years, apparently benefitting from a protective hydrodynamic oil film, was waiting to be properly explained. Although some understanding of the basics of EHL had been provided by Grubin/Ertel, it was Dowson and Higginson who conceived a novel, consistent numerical approach to solving the full governing equations for a line contact, which they published in their classic paper of 1959. Without doubt the paper was the starting point for a flurry of interest in EHL that continues to this day, and from which numerous international research groups drove forward their own work on extending the understanding of EHL, both theoretically and by experimental studies. Very early in his EHL research Dowson knew that a conventional forward/iterative approach to the solution of the basic equations was of no use. His invention of the inverse hydrodynamic approach was the key to solving the line contact under realistic conditions. Following workers wanted to tackle EHL point contacts (as found in ball bearings) in which the inverse method is far more difficult to apply in a consistent, robust solver. This led to

both Dowson and others adopting new, powerful methods of solving heavily loaded point contacts such as the multi-grid and differential deflection techniques. Using these techniques all kinds of EHL contacts have been successfully studied under realistic engineering conditions by numerous groups across the globe.

Gearing, which is the focus of the present article, has, in particular, benefitted from the ground-breaking work carried out by Duncan Dowson, and by many other subsequent contributors. In our own EHL work we have concentrated on the understanding and performance of practical gearing devices, examples of which are summarised in Section 2. Gear applications continue to be very challenging because gear teeth operate at high contact pressures and, unlike the polished smoothness of rolling element bearings, they generally have calculated smooth surface films that are of the same order, and even thinner, than the height of roughness features. Duncan Dowson's fundamental contribution to EHL theory provided the foundation that has led directly to most of the analytical advances made in this field - and will continue to do so.

## References

- [1] Crowe, T.A., Some recent advances in mechanical engineering on shipboard, Proc Inst. Mech. Engrs., **158**, (1948), 264-277
- [2] Martin, H.M., Lubrication of gear teeth, Engineering (London), **102** (1916), 119-121.
- [3] Grubin, A.N., Central Scientific Research Institute for Technology and Mechanical Engineering, Book No. 30, Moscow, 1949. DSIR Translation No. 337.
- [4] Dowson, D. and Higginson, G.R., A numerical solution to the elastohydrodynamic lubrication problem. J. Mech. Eng. Sci, **1**, (1959) 6-15.
- [5] Dowson, D. and Higginson, G.R. Reflections on early studies of elastohydrodynamic lubrication. Proc IUTAM Symposium on Elastohydrodynamics and micro-elastohydrodynamics. RW Snidle and HP Evans (eds), Springer, 2006, 3-21
- [6] Petrusevich, A.I., Fundamental conclusions from the contact hydrodynamic theory of lubrication, Izv Uzbekist, Fil. Acad. Nauk, SSSR (OTN), **2**, 209-223.
- [7] Dowson, D. and Higginson, G.R., The Effect of material properties on the lubrication of elastic rollers, J. Mech. Engng. Sci. **2** (3), 188-194.
- [8] Hamilton, G.M. and Moore, S., Deformation and pressure in an elastohydrodynamic contact, Proc. R. Soc. Lond. **A322**, (1971), 313-330
- [9] Dowson, D. and Higginson, G.R. New roller bearing lubrication formula, Engineering, **192** (4972), 158-159

- [10] Dowson, D. and Higginson, G.R. *Elastohydrodynamic Lubrication*, 1966 Pergamon, Oxford)
- [11] Dowson, D. and Toyoda, S., A central film thickness formula for elastohydrodynamic line contacts, *Proc. 5<sup>th</sup> Leeds-Lyon Symposium on Tribology*, Mechanical Engineering Publications, Bury St Edmunds UK (1979), 60-65
- [12] Dyson, A., Naylor, H, and Wilson, A. R., The measurement of oil film thickness in elastohydrodynamic contacts, *Proc. IMechE* **180** (3B) (1965) 119-134.
- [13] American Society for testing and materials (ASTM), 1998. Standard Viscosity-Temperature Charts for liquid Petroleum Products. Designation D341-93, Pp 002-006.
- [14] Jackson, A. 1992. Mobil EHL guidebook. Mobil Oil Corporation, Fairfax VA. 4<sup>th</sup> edition.
- [15] Wu, C.S. et al. 1989. Development of a Method for the Prediction of Pressure-Viscosity Coefficients of Lubricating Oils Based on Free-Volume Theory. *Journal of Tribology* 111(1), pp. 121-128.
- [16] Crook, A. W., “The Lubrication of Rollers III. A Theoretical Discussion of Friction and the Temperatures in the Oil Film,” *Phil. Trans. R. Soc.*, **A254**, (1961), 237-258.
- [17] Hu, J. The kinematic analysis and metrology of cylindrical worm gearing, PhD thesis, University of Newcastle upon Tyne 1997.
- [18] Sharif, K.J., Kong, S., Evans, H.P. and Snidle, R.W., Contact and analysis of worm gears Part 1: theoretical formulation, *Proc. Instn. Mech. Engrs, Part C: Journal of Mechanical Engineering Science*, **215** (2001), 817-830
- [19] Sharif, K.J., Kong, S., Evans, H.P. and Snidle, R.W., Contact and analysis of worm gears Part 2: results, *Proc. Instn. Mech. Engrs, Part C: Journal of Mechanical Engineering Science*, **215** (2001), 831-846
- [20] Barragan de Ling, F dM, Evans, H.P., and Snidle, R.W., Thrust cone lubrication Part 1: elastohydrodynamic analysis of conical rims, *Proc. Instn. Mech Engrs, Part J: Journal of Engineering Tribology*, **210** (1996), 85-96
- [21] Barragan de Ling, FdM, Evans, H.P., and Snidle, R.W., Thrust cone lubrication Part 2: elastohydrodynamic analysis of crowned rims, *Proc. Instn. Mech Engrs, Part J: Journal of Engineering Tribology*, **210** (1996), 97-105
- [22] Jamali, H. U., Sharif, H. J., Evans, H. P. and Snidle, R. W. The Transient Effects of Profile Modification on Elastohydrodynamic Oil Films in Helical Gears, *Tribology Transactions*, 58:1, (2015) 119-130, DOI:10.1080/10402004.2014.936990
- [23] A. Clarke, H.U. Jamali, K. J. Sharif, H.P. Evans, R. Frazer, B. A. Shaw. Effects of profile errors on lubrication performance of helical gears, *Tribology International* , (2017) 10.1016/j.triboint.2017.02.0034, 111, pp184-191
- [24] Fatemi, A. and Socie, D. F. A critical plane approach to multiaxial fatigue damage including out-of-phase loading. *Fatigue Fract. Eng. Mater. Struct.*, 1988, **11**,149–165.
- [25] Qiao, H., Evans, H. P. and Snidle, R. W. Comparison of fatigue model results for rough surface elastohydrodynamic lubrication, *Leeds-Lyon Symposium on Tribology, Lyon* , (2007) *Proc. Instn. Mech. Engrs Part J, Jn of Engng Tribology*, Vol 222, pp 381-393, 2008.